

Synthesis and Structure-Activity Relationship of Several Aromatic Ketone-Based Two-Photon Initiators

ZHIQUAN LI,¹ MARTON SIKLOS,¹ NIKLAS PUCHER,¹ KLAUS CICHA,² ALIASGHAR AJAMI,³ WOLFGANG HUSINSKY,³ ARNULF ROSSPEINTNER,⁴ ERIC VAUTHEY,⁴ GEORG GESCHEIDT,⁵ JÜRGEN STAMPFL,² ROBERT LISKA¹

¹Institute of Applied Synthetic Chemistry, Division of Macromolecular Chemistry, Vienna University of Technology, Getreidemarkt 9/163/MC, 1060 Vienna, Austria

²Institute of Materials Science and Technology, Vienna University of Technology, Favoritenstrasse 9-11, 1040 Vienna, Austria

³Institute of Applied Physics, Vienna University of Technology, Wiedner Hauptstrasse 8, 1060 Vienna, Austria

⁴Department of Physical Chemistry, University of Geneva, 30, Quai Ernest Ansermet CH-1211 Geneva 4, Switzerland

⁵Graz University of Technology, Institute of Physical and Theoretical Chemistry, Stremayrgasse 9, 8010 Graz, Austria

Received 8 April 2011; accepted 25 May 2011

DOI: 10.1002/pola.24806

Published online 14 June 2011 in Wiley Online Library (wileyonlinelibrary.com).

ABSTRACT: Several novel aromatic ketone-based two-photon initiators containing triple bonds and dialkylamino groups were synthesized and the structure-activity relationships were evaluated. Branched alkyl chains were used at the terminal donor groups to improve the solubility in the multifunctional monomers. Because of the long conjugation length and good coplanarity, the evaluated initiators showed large two-photon cross section values, while their fluorescence lifetimes and quantum yields strongly depend on the solvent polarity. All novel initiators exhibited high activity in terms of two-photon-induced microfabrication. This is especially true for fluorenone-based derivatives, which displayed much broader processing windows than well-known highly active

initiators from the literature and commercially available initiators. While the new photoinitiators gave high reactivity in two-photon-induced photopolymerization at concentration as low as 0.1% wt, these compounds are surprisingly stable under one photon condition and nearly no photo initiation activity was found in classical photo DSC experiment. © 2011 Wiley Periodicals, Inc. *J Polym Sci Part A: Polym Chem* 49: 3688–3699, 2011

KEYWORDS: laser-induced polymers; NLO; photochemistry; photopolymerization; radical polymerization; two-photon absorption photoinitiator

INTRODUCTION Two-photon-induced photopolymerization (TPIP) has been intensively studied recently as the interest in the fabrication of smaller features for nanotechnology, information technology, and other industries requiring high precision has significantly increased.^{1–5} With this unique process, it is possible to produce complex 3D structures with spatial resolution (120 nm) below the diffraction limit of the utilized wavelength.⁶

TPIP is a solid free-form fabrication technique where a resin, which contains mainly a multifunctional acrylate-based monomer and a photoinitiator (PI), is cured inside the focal point of a femtosecond pulsed laser. To obtain an efficient and clean polymerization and therefore high-quality structures, a highly active two-photon absorption (TPA) PI plays a key role.

Originally commercially available radical PIs were usually used in the initial stages of TPIP research.^{7,8} As these PIs have rather low cross sections (σ_{TPA}) and therefore poor absorption behavior,⁹ high excitation power and long exposure time,

which often result in damage to the polymeric structures are usually required. Therefore, great efforts were made to improve the two-photon sensitivity. In the last decades, plenty of chromophores with large σ_{TPA} were synthesized.¹⁰ However, most of the reported chromophores exhibit high fluorescence yields as desirable for fluorescence imaging applications.^{11,12} On the other hand, to be effective as a TPA initiator, low fluorescence quantum yields are preferred as this leads to a higher population of the triplet state (triplet quantum yield), which is usually the active state of the initiators producing radicals or ions for initiating the polymerization.¹³ Thus, a large σ_{TPA} value combined with a high photoreactivity just like for normal one-photon initiators seems to be the goal to achieve.

To design an ideal molecular structure with a high σ_{TPA} value, several intramolecular key features have been identified.¹⁴ To utilize intramolecular charge-transfer as the “driving force” for TPA,^{15,16} electron-donor and electron-acceptor groups are required. In addition, coplanar π conjugated

Additional Supporting Information may be found in the online version of this article.

Correspondence to: R. Liska (E-mail: robert.liska@tuwien.ac.at)

Journal of Polymer Science Part A: Polymer Chemistry, Vol. 49, 3688–3699 (2011) © 2011 Wiley Periodicals, Inc.

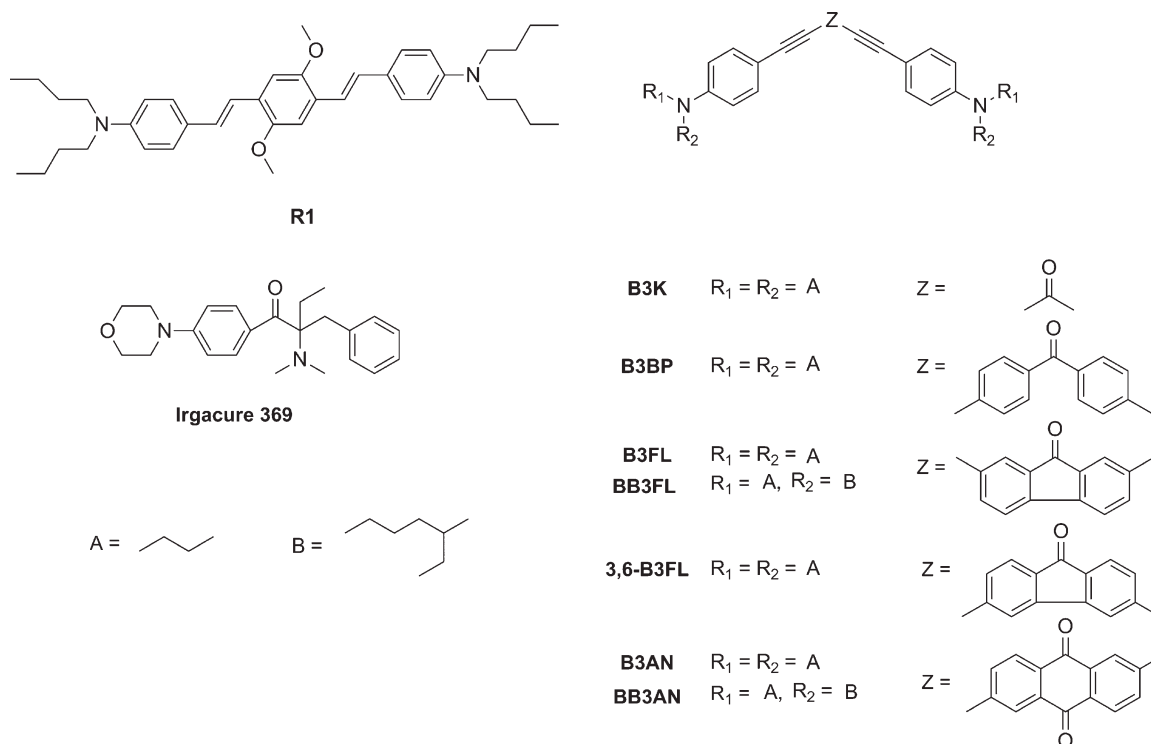


FIGURE 1 New TPA PIs and reference compounds.

bridges which lead to states with extended charge separation,^{17,18} are critical in enhancing the efficiency of intramolecular charge transfer. Usually double bonds, due to their simple synthetic accessibility, are used in the backbone of the PIs to extend the conjugation length although the so obtained σ_{TPA} is normally lower than that of the triple-bond-containing counterparts.^{19,20} However, double bonds tend to attenuate the desired photochemical processes by *cis-trans* isomerization.

Recently, we have reported on the successful syntheses and evaluation of a series of radical PIs optimized for TPIP processes.²¹ 1,5-Bis(4-(*N,N*-dibutylamino)phenyl) penta-1,4-diyne-3-one (**B3K**) containing a triple-bond π -bridge and a carbonyl group as electron withdrawing functional group serves as a highly sensitive and efficient TPA PI in comparison with typical one-photon UV PIs and other very potent two-photon initiators well known from literature,²² such as E,E-1,4-bis[4'-(*N,N*-di-*n*-butylamino) styryl]-2,5-dimethoxybenzene (**R1**) and E,E-1,4-bis-[4'-(*N,N*-di-*n*-butylamino)styryl]benzene (**R2**). Nicely shaped structures and broad processing windows can be obtained with PI concentrations as low as ~ 0.05 wt %. It is worth to mention that compared to **R1**, which shows strong fluorescence, the triple bond containing ketone-based PIs either do not show any or an extremely weak ($\Phi_{\text{em}} < 5 \times 10^{-3}$) fluorescence emission. This is rationalized by an efficient intersystem crossing to the excited triplet state.²³

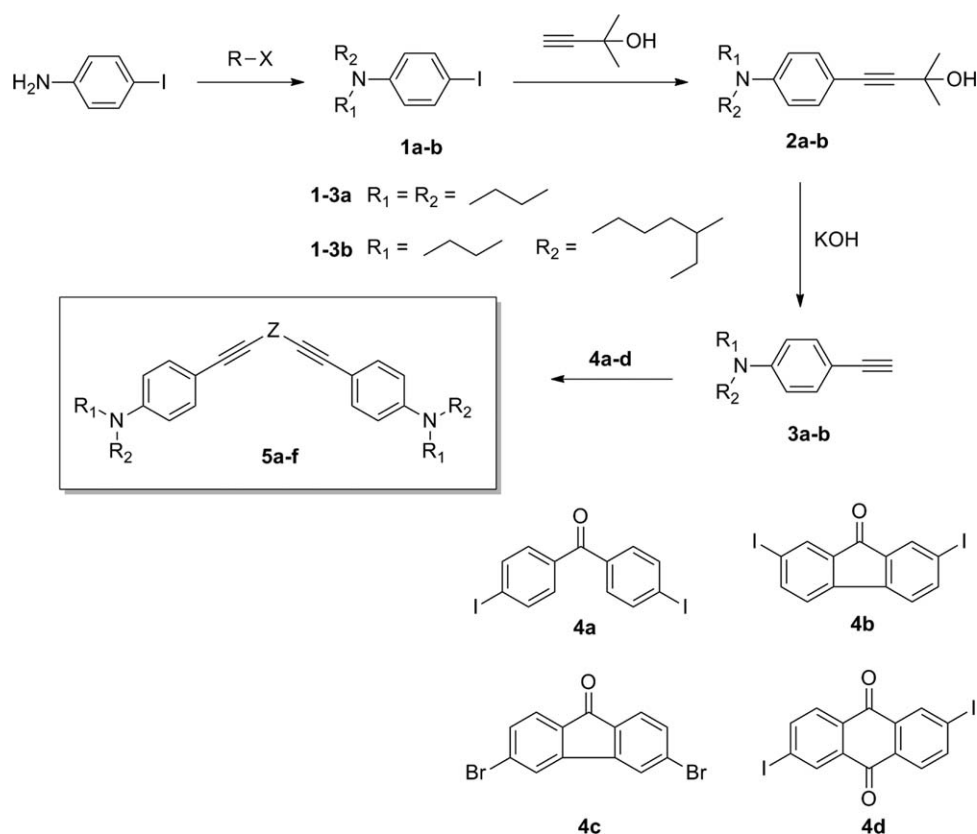
Based on the molecular structure of **B3K** containing triple bonds and cross-conjugated D- π -A- π -D lead structures, several aromatic ketone-based TPA PIs (Fig. 1) were investi-

gated in this article. To study structure-activity relationships, we used different aromatic ketones (benzophenone, fluorenone and anthraquinone) as acceptors in the central part of the π bridge and dialkylamino groups as electron-donor moieties.

Compared to **B3K**, the benzophenone-based initiator **B3BP** exhibits a longer conjugation length of the whole π system and therefore a higher σ_{TPA} can be expected. Structure-activity relationship tests in the recent literature showed that benzophenone-bearing dyes exhibit much larger σ_{TPA} than their analogues without a benzophenone unit.²⁴

Additionally, aromatic ketones with stereorigid carbon skeleton (**B3FL**, **3,6-B3FL**, and **B3AN**) were chosen to ensure good coplanarity, thus facilitating the intermolecular charge transfer process, which is critical in enhancing σ_{TPA} . Anthraquinone was used because of its excellent electron accepting ability and because its 2-, 6-positions can be easily modified by introducing π conjugated systems with electron donor groups resulting in a D- π -A- π -D (A = electron acceptor and D = electron donor) type molecule. Recently, a double-bond containing anthraquinone compound was synthesized and exhibited a large two-photon cross section value of 1635 GM ($1 \text{ GM} = 10^{-50} \text{ cm}^4 \text{ s photon}^{-1}$) at 800 nm, as well as low fluorescence quantum yield.¹³

B3FL was selected because 2,7-substituted fluorene cores are known to exhibit high thermal and photochemical stability.²⁵⁻²⁷ Furthermore, the electron-withdrawing carbonyl group at C-9 stabilizes the LUMO of fluorene, making it remarkably electrophilic.²⁸ Substitution at positions 3 and 6



SCHEME 1 Reaction scheme for the synthesis of the new TPA PIs.

theoretically offers good electronic communication through the entire fluorenone skeleton.²⁸ To investigate the effect of different substituted positions on structure-reactivity relationships, 2,7- and 3,6-substituted fluorenone compounds were synthesized and are being discussed in this article.

Moreover, the solubility in the monomers is an important issue for the efficiency of TPA initiators. This issue has been addressed by the introduction of branched-alkyl chains at the end of the amino moieties, as in **BB3FL** and **BB3AN**.

For comparison, the highly efficient TPA PI **R1**, well-known from the literature,²² and **Irgacure 369** (a typical commercially available one-photon PI, that is, also frequently applied in TPIP) were tested. For the characterization of the initiators, UV-vis absorption and emission measurements were carried out. Two photon cross-section measurements via z-scan, as well as TPIP structuring tests were performed to evaluate the TPA properties of the initiators. Ideal building parameters for each initiator were determined by changing the laser intensity, the feed rate, and the shape size using the same molar PI concentrations.

RESULTS AND DISCUSSION

Synthesis

For the synthesis of the new initiators (Scheme 1), there are two key intermediates **3a** and **3b** based on the *p*-amino aryl alkyne group containing different alkyl chains at the N-atom. These intermediates can be prepared by Sonogashira cou-

pling reactions of the appropriate iodo dialkylamino benzenes with either (trimethylsilyl)acetylene or 2-methyl-3-butyn-2-ol followed by a subsequent cleavage of the protection group in two steps^{29,30} or a Wittig-type one pot synthesis starting from the corresponding aldehydes.³¹ Although we have previously proven that both methods are suitable to obtain the terminal aryl acetylenes in high yields,²¹ the former method was chosen because various alkyl chains could be easily realized for alternative PIs in further studies, while the counterpart aldehyde compounds are not always commercially available.

The 4-iodobenzeneamine derivatives (**1a-b**) required for the Sonogashira reaction had to be synthesized via alkylation of 4-iodobenzeneamine with different alkyl halides. The butyl derivative **1a** was obtained with 1-iodobutane in high yields (78%). For economical reasons, 3-(bromomethyl)heptane was used instead of its iodo analogues to prepare branched precursor in the presence of potassium iodide and a phase transfer catalyst (tetrabutylammonium bromide). As a second substitution with the branched alkyl chain exhibited quite low yield (less than 15% from GC-MS) due to the steric hindrance, one butyl group was used instead to give **1b** in 60% yield.

The reaction of these 4-iodobenzeneamine derivatives with 2-methyl-3-butyn-2-ol under Sonogashira conditions gave the protected alkyne products **2a-b** in yields between 83 and 88%. Finally, by deprotection under basic conditions the terminal alkynes **3a-b** were obtained in good yields (80–87%).

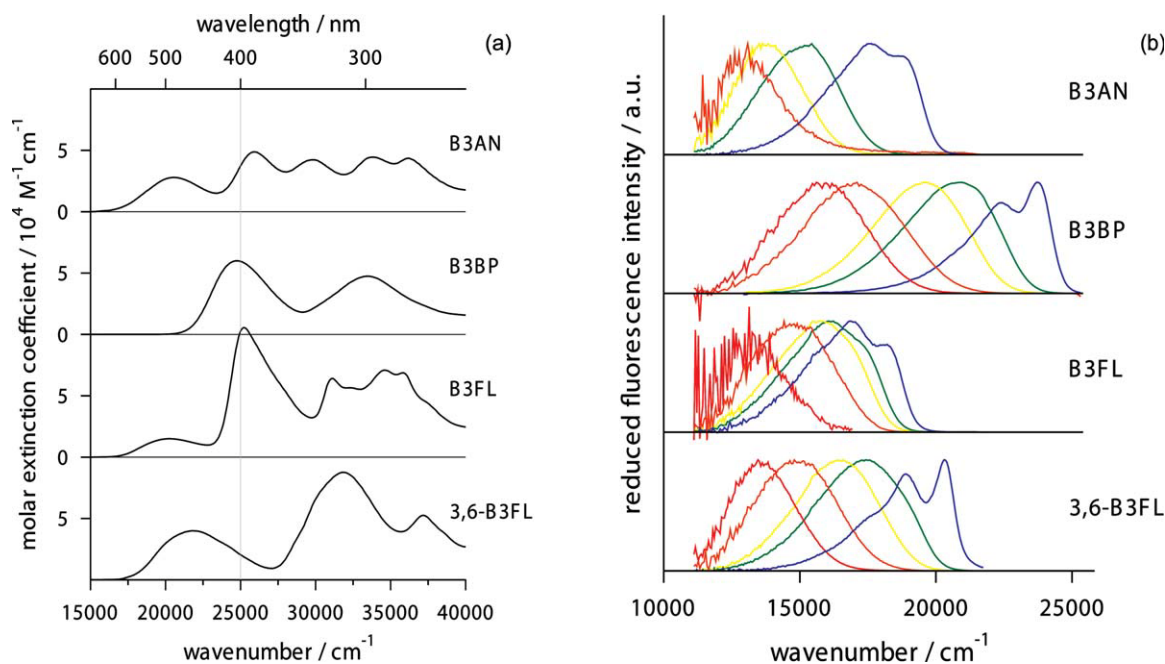


FIGURE 2 (a) Absorption spectra of 3,6-B3FL, B3FL, B3AN, and B3BP in dichloromethane. The half wavelength of the TPA cross-section measurements (400 nm) is shown as vertical gray line. (b) Reduced fluorescence spectra ($I(v)/v^3$) of 3,6-B3FL, B3FL, B3AN, and B3BP in cyclohexane (blue), butyl ether (green), ethyl ether (yellow), butyl acetate (orange, for B3BP propyl acetate) and dichloromethane (red). [Color figure can be viewed in the online issue, which is available at wileyonlinelibrary.com.]

The dihalide aromatic ketones **4a-d** for the coupling reaction with terminal alkynes **3a-b** could be prepared from the corresponding aromatic compounds via direct iodination or a subsequent oxidation in one pot reactions with the reaction yield ranging from 60 to 75%.³²⁻³⁴ 3,6-Dibromo-fluorenone was synthesized from the light-induced bromination of phenanthrene-9,10-dione followed by elimination under basic condition.^{35,36} Multiple recrystallizations in DMSO must be performed to remove trace amounts of 3,6-dibromophenanthrene-9,10-dione, which is detrimental toward efficient Sonogashira couplings.²⁸

On the basis of these intermediates, the final PIs were obtained by Sonogashira coupling reactions of the terminal alkyne derivatives with different aromatic ketone halides with yields of 36–57%.

Spectroscopy

Figure 2(a) depicts the absorption spectra of **B3AN**, **B3BP**, **B3FL**, and **3,6-B3FL** in dichloromethane (also Table 1 for some prominent values of the extinction coefficient). All TPIPs evaluated do not exhibit any linear absorption beyond 600 nm, which could thus interfere at the wavelength used in the z-scan experiments and the two-photon polymerization microfabrication. The absorption spectra of these novel PIs exhibit a low energy absorption band, which appears at significantly lower energies than those of either the parent central accepting molecule (i. e. fluorenone, benzophenone, anthraquinone) or the 4-(dimethylamino)ethynylbenzene donor moiety.³⁷ This “new” band is rather intense, with its maximum molar decadic extinction coefficient, ϵ , being in the range from 10^4 to $5 \times 10^4 \text{ M}^{-1} \text{ s}^{-1}$, and shows a slight hyp-

sochromic shift with increasing solvent polarity (Table 2). A thorough solvatochromic analysis of these absorption bands, for example, of Lippert-Mataga (LM) type, is, however obscured by the fact that the absorption band is rather broad, slightly changes shape with the solvent (not shown) and overlaps with the adjacent transitions. Any attempts of performing a LM analysis using simply the maxima of the absorption band resulted in suboptimal (i.e., nonlinear) LM plots. This might indicate, that the nature of the transition is changing with the solvent, from a mainly local excitation in apolar solvents to a partial charge transfer absorption in polar solvents (or at least the amount of charge transfer character is changing).

Inspection of Figure 2(b) and Table 2 shows that the situation is only slightly better concerning the interpretation of the emission spectra. The 4 TPIPs investigated (**B3AN**, **B3BP**, **B3FL**, and **3,6-B3FL**) show a relative intense and structured fluorescence in apolar cyclohexane. By increasing the solvent

TABLE 1 Molar Extinction Coefficients of 3,6-B3FL, B3FL, B3AN, and B3BP in Dichloromethane for the Two Lowest Energy Absorption Maxima and the Half Wavelength of the TPA Cross-Section Measurements (400 nm)

Substance	λ (nm)	$10^{-3}\epsilon$ ($\text{M}^{-1} \text{ cm}^{-1}$)
B3AN	485/400/387	28/38/50
B3BP	405/400/300	60/60/50
B3FL	495/400/396	15/100/105
3,6-B3FL	460/400/315	40/20/85

TABLE 2 Basic Photophysical Properties of 3,6-B3FL, B3FL, B3AN, and B3BP in Six Solvents at 25 °C

Solvent	ϵ	n	ν_f (eV)	ν_a (eV)	$\phi_f \cdot 10^{-3}$	τ (ns)
B3AN						
CX	2.01	1.4235	2.18	2.67	520	4.3
BE	3.08	1.3968	1.87	2.64	130	2.3
EE	4.20	1.3495	1.71	2.66	17	0.6
BA	5.01	1.3918	1.62	2.61	0.7	–
DC	8.93	1.4210	–	2.53	–	–
B3BP						
CX	2.01	1.4235	2.95	3.16	70	0.1
BE	3.08	1.3968	2.57	3.15	340	1.7
EE	4.20	1.3495	2.43	3.16	430	1.8
PA	6.00	1.3828	2.11	3.13	230	1.7
DC	8.93	1.4210	1.96	3.05	160	1.8
B3FL						
CX	2.01	1.4235	2.10	2.61	440	4.6
BE	3.08	1.3968	1.99	2.57	150	2.3
EE	4.20	1.3495	1.98	2.57	110	2.0
BA	5.01	1.3918	1.84	2.54	15	0.5
PA	6.00	1.3828	1.80	2.52	11	0.4
DC	8.93	1.4210	1.65	2.49	0.7	–
3,6-B3FL						
CX	2.01	1.4235	2.52	2.93	210	0.8
BE	3.08	1.3968	2.17	2.87	650	3.6
EE	4.20	1.3495	2.04	2.83	680	4.1
BA	5.01	1.3918	1.84	2.77	90	0.9
PA	6.00	1.3828	1.81	2.76	44	0.9
DC	8.93	1.4210	1.69	2.68	12	0.3

The properties comprise the energies of the maximum of the reduced fluorescence spectrum ($I(\nu)/\nu^3$), ν_f , the lowest energy maximum of the reduced absorption spectrum ($\epsilon(\nu)/\nu$), ν_a , the fluorescence quantum yield and the fluorescence lifetime. Additionally the dielectric constant, ϵ , and refractive index, n , of the solvent are given.

CX, cyclohexane; BE, butyl ether; EE, ethyl ether; BA, butyl acetate; PA, propyl acetate; DC, dichloromethane.

polarity (from cyclohexane to dichloromethane), the emission spectra undergo more (for **3,6-B3FL** and **B3BP**) or less (**B3FL**) strong bathochromic shifts in the range of 0.5–1 eV. Additionally the emission spectra lose their vibronic structure upon increasing the solvent polarity, with their bandshape resembling more and more that of a pure charge transfer transition. Since these trends are more or less prominent for certain TPIPs, it is worth emphasizing their differences: For both **B3AN** and **B3FL**, lifetime and emission quantum yield decrease monotonously with increasing solvent polarity. For **3,6-B3FL** the emission quantum yield and lifetime pass through a maximum for the ethers but hold a smaller value in cyclohexane. For **B3BP**, whose emission and absorption spectrum are also at higher energies than for the other PIs, the quantum yield and lifetime show no pronounced dependence with solvent polarity, except for the fact that these values in cyclohexane are rather low.

On the basis of the present data, which comprise only steady-state and subnanosecond time-resolved emission experiments, the following tentative conclusions may be drawn. A charge transfer state is populated either via direct excitation, or indirectly, via excitation of a locally excited state.³⁸ The current data does not allow speculations of possible populations of the triplet state of the PIs. However femtosecond time resolved transient absorption and emission spectroscopy are currently being performed to help shed light onto the photophysics and possible mechanism(s) of photoinitiation for these TPIPs.

TPA Cross Section

To investigate the TPA properties of the new PIs, an open aperture z-scan analysis was performed to determine the TPA cross section at 800 nm. THF was used as solvent for the TPA characterization of all compounds. A nonrecycling flow cell geometry was used for the measurements because of the strong photodegradation of some PIs during the tests (especially the ketone-based PIs). This phenomenon was also described by Schafer et al.⁹ and was furthermore described as an indicator for an effective two-photon initiator. In the Supporting Information, the photo-degradation of **BB3FL** is shown as a representative example at two different z-scans: without flow and with 4 mL/h flow rate. The results indicated that a flow rate of 4 mL/h is sufficient for all PIs to wash the irradiated sample out of the focal volume in a reasonable time.

The experimental data were fitted using the adopted equations of Sheik-Bahae et al.³⁹ To obtain the TPA cross section (σ) [Fig. 3(a)]. To exclude excited-state absorption and to verify that a pure σ is determined, the measurements were repeated at different peak intensities and the calculated parameter q_0 scales linearly with intensity [Fig. 3(b)].³⁹ All calculated σ values are given in Table 3.

The cross section value of the reference compound **R1** is in good agreement with our previous result²¹ and the literature,²² verifying the reliability of the experimental setup. With longer conjugation length, benzophenone-based initiator **B3BP** showed a larger cross section value than **B3K** of 238 GM, which is almost equal to that of **R1**. By changing the acceptor group in **B3BP** from a benzophenone group to an anthraquinone moiety as in **B3AN**, the value decreased to 235 GM. The reduction may be due to the relatively lower absorption in one-photon spectra at about 400 nm, which indicates that the TPA peaks in TPA spectra are shifted in wavelength away from 800 nm. As expected, the substitution of the butyl group at the amine by branched alkyl chains alters the two photon cross section only marginally.

Interestingly, the 3,6-substituted fluorenone-based PI, which theoretically should facilitate an intramolecular electron transfer process, exhibits a lower cross section value compared to the 2,7-substituted analogue **B3FL**. An explanation can be given by the red-shift-induced low TPA absorption at the given wavelength. Among the aromatic ketone derivatives, **B3FL** had the highest TPA cross section value with 440 GM. One reason is the excellent coplanarity of the stereo rigid fluorenone carbon

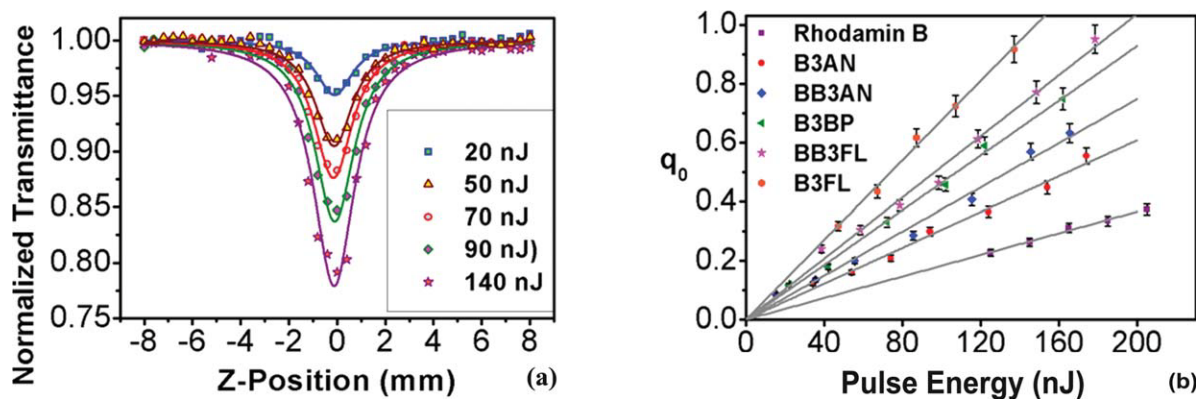


FIGURE 3 (a) Experimental z-scan data (dots) and fitting curves (full lines) for B 3FL at different pulse energies. (b) q_0 plotted versus intensity for the investigated PIs and an example for standard measurement and fitting data. [Color figure can be viewed in the online issue, which is available at wileyonlinelibrary.com.]

frame and the suitably strong absorption around 400 nm, which ensured the considerable TPA at 800 nm.

Determination of the TPA cross section gives only information about the absorption behavior (similar to the extinction coefficient, ϵ , of one-photon absorption in Lambert-Beer's law). Thus, TPIP structuring tests were performed to further characterize the new PIs.

TPIP Structuring Test

To estimate the activity of the PIs, defined test structures (lateral dimension: $50 \times 50 \mu\text{m}$, $10 \mu\text{m}$ hatch-distance, $0.7 \mu\text{m}$ layer-distance, 20 layers) were written into the monomer formulation by means of TPIP. The laser intensity was screened in a range of 1–32 mW (measured after passing the $100\times$ microscope objective). A 1:1 mixture of Trimethylolpropane triacrylate (TTA) and ethoxylated (20/3)-trimethylolpropane triacrylate (ETA) as an acrylate-based test resin with the same molar PI concentration of 6.3×10^{-6} mol PI/g resin was used, since good results had been previously achieved under these conditions.⁴⁰

The different color of the bars and their corresponding numbers in Figure 4 indicate the quality of the structures. At write speeds beyond the ideal processing window, the initiation threshold is not reached and incompletely connected structures are obtained after the standard post processing

TABLE 3 TPA Cross Section Values of PIs in THF by z-Scan Measurement at 800 nm

PI	σ_{TPA} (GM)
R1	328
B3K ²¹	238
B3BP	336
B3FL	440
B3AN	235
3,6-B3FL	308
BB3FL	385
BB3AN	250

procedure. Above that, class 1 defines excellent structures with fine hatch-lines and class 2 good structures with thick hatch-lines (compared to class 1) or slightly contorted structures (Fig. 5). Generally, broader “perfect” processing windows (class 1 and 2) and lower laser intensities are desired in terms of high throughput in mass production because this allows a splitting of the initial laser beam for parallel processing with multiple laser heads at high feed rates, while thermally induced decomposition of the material can be avoided. Samples rated as class 3 have shapes that can be identified but with small mistakes (e.g., holes, exploded regions caused by overexposure). Parts structured with laser intensities rated as class 4 no longer showed acceptable results. The shapes are no longer identifiable with completely missing walls and/or vast holes.

In our measurements, the well-known initiator from the literature **R1** can be used to build nicely shaped structures at low laser intensities. On the other hand, the commercially available PI **Irgacure 369** showed no good results at 800 nm at the given PI concentration (6.3×10^{-6} mol PI/g resin), which is in good agreement with the low TPA cross section.⁹ However, by increasing the concentration of **Irgacure 369** up to 1 wt %, nice shaped structures could be obtained at 600 nm excitation.²¹ The same concentration effect was also observable when using the presented initiators.

The benzophenone-based initiator **B3BP** gives nice structures at similarly low laser intensities as **R1**, but its ideal processing window is significantly smaller. By changing the acceptor group in **B3BP** from a benzophenone group to an anthraquinone moiety as in **B3AN**, the solubility was dramatically decreased. In the structuring tests, we were not able to obtain any good results with **B3AN** due to its poor solubility (data not shown). The introduction of branched-alkyl chains at the end of the amino moieties of the anthraquinone-based initiator **BB3AN** could, to some extent, resolve the solubility problem. However, high laser intensities are required to obtain good structures in a small area. This might be explained by the relatively small TPA cross section and the significantly lower solubility in the resin.

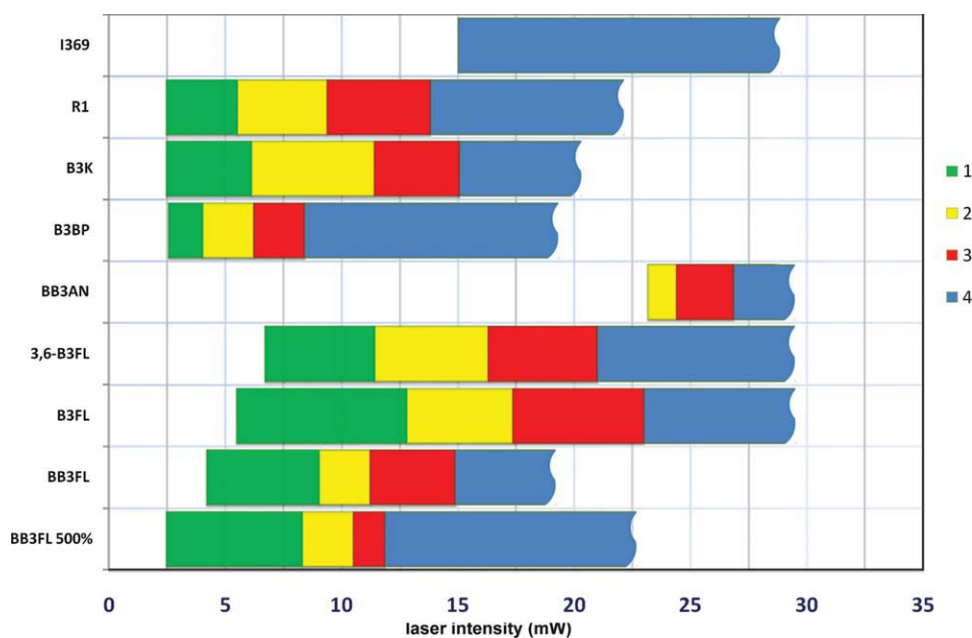


FIGURE 4 PI TPIP screening tests (PI concentration: 6.3×10^{-6} mol PI/g resin).

The fluorenone-based initiators (**3,6-B3FL**, **B3FL**, and **BB3FL**) showed very good results in these tests. The ideal processing windows are broader than that of the references, but the required laser intensities are slightly higher. Despite the lower cross section compared to that of **B3BP**, the ideal window of **3,6-B3FL** is much broader. This might be explained by the stereo rigidity of the carbon frame of fluorenone, which increases the coplanarity of the entire molecule and thus facilitates the electron transfer process (the mechanism of photopolymerization is currently under investigation). The triple bonds attached at the 2- and 7-positions of **B3FL**, exhibit much broader ideal processing windows than those of **3,6-B3FL**, which is in good agreement with the z-scan values. By changing the alkyl side chains from butyl to branched alkyl chains of **BB3FL**, the ideal processing win-

dows (class 1 and 2) became smaller. The difference may be explained by the lower migration ability of the PI with the increase of its molecule size. The lower laser intensity required for **BB3FL** might be attributed to the increased solubility. It is worth mentioning that the introduction of branched-alkyl chains significantly improved the solubility of the fluorenone-based PIs. Laser intensities as low as 2.47 mW could be used to obtain nice structures with fairly high concentrations (3.2×10^{-5} mol PI/g resin) of **BB3FL**. **B3FL** turned out to be the best performing initiator in our tests having the broadest ideal structuring process window at low concentration (6.3×10^{-6} mol PI/g resin) and good solubility in the resin.

The tests were repeated also with lower molar PI concentrations to determine the lowest possible PI concentration under these conditions. For the lower concentration (1.6×10^{-6} mol PI/g resin, 0.1% wt of **B3FL**) the results for all initiators are very similar to those at higher concentration, with the only difference having a slight shift of the ideal processing window towards higher laser intensities.

Additionally, more complex 3D structures (Fig. 6) were inscribed into the material volume using **B3FL** (6.3×10^{-6} mol PI/g resin) as initiator. These shapes demonstrate perfectly the advantages of TPIP compared to other rapid prototyping techniques. High spatial resolution, which is otherwise inaccessible, and complex 3D structures with massive overhangs such as the St. Stephen's Cathedral of Vienna [Fig. 6(a)] can be easily obtained.

EXPERIMENTAL

Materials

All reagents were purchased from Sigma-Aldrich, Fluka, and ABCR and were used without further purification. The solvents were dried and purified by standard laboratory

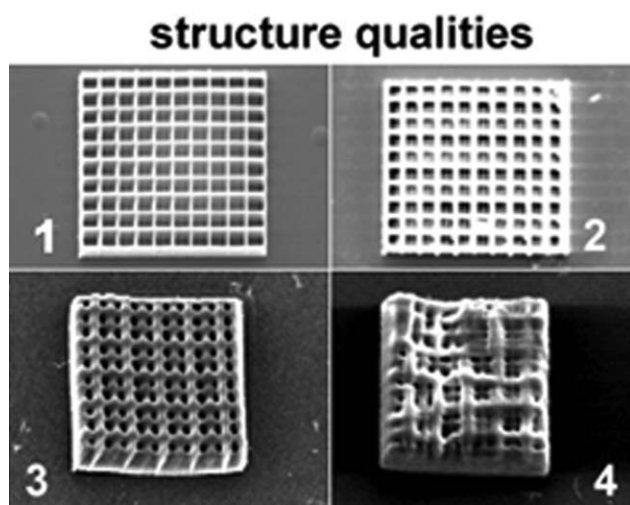


FIGURE 5 Classification of the structures by the typical quality of their shapes.

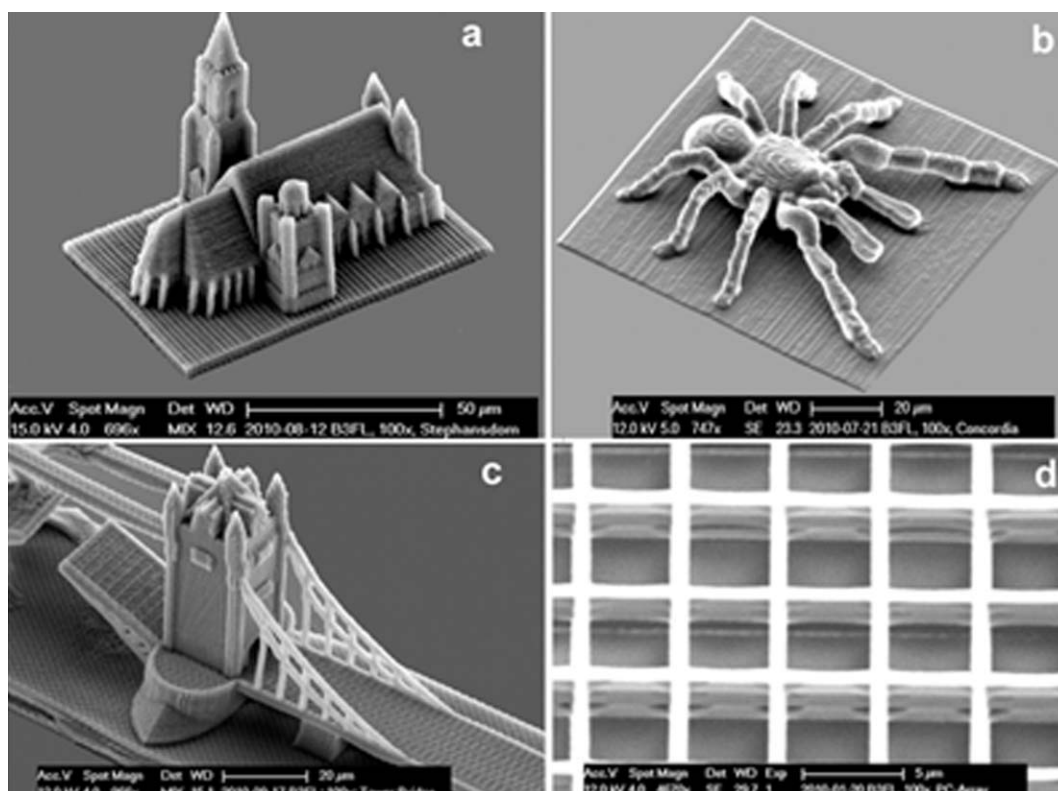


FIGURE 6 3D structures (resin ETA/TTA 1:1, B3FL as initiator): (a) St. Stephen's Cathedral; (b) Tarantula Spider; (c) detail of the London Tower Bridge; (d) detailed view of the woodpile structure.

methods or were dried over Al_2O_3 cartridges. Trimethylolpropane triacrylate (TTA, Genomer 1330) and ethoxylated (20/3)-trimethylolpropane triacrylate (ETA, Sartomer 415) were received as a gift from Rahn and Sartomer, respectively. Petroleum ether (PE) refers to the fraction boiling in the range 40–60 °C. Column chromatography was performed with conventional techniques on VWR silica gel 60 (0.040–0.063 mm particle size). Aluminum-backed silica gel plates were used for TLC analyses.

Synthesis

N,N-dibutyl-4-iodobenzeneamine (**1a**),²¹ Bis(4-iodophenyl)-methanone (**4a**),³⁴ 2,7-diiodo-9H-fluoren-9-one (**4b**),³³ 3,6-dibromophenanthrene-9,10-dione,³⁶ 3,6-dibromo-9H-fluoren-9-one (**4c**),³⁵ 2,6-diiodo-9,10-anthraquinone (**4d**)³² were prepared according to the literature. A detailed synthesis procedure is also given in the Supporting Information.

N-Butyl-*N*-(2-ethylhexyl)-4-iodoaniline (**1b**)

To a solution of 21.91 g (100 mmol) of 4-iodoaniline in 300 mL degassed dry DMF under argon atmosphere, 50 mL (300 mmol) of 3-(bromomethyl)heptane, 41.46 g Na_2CO_3 powder (300 mmol), 8.31 g (50 mmol) of potassium iodide and 2 g (6 mmol) tetrabutylammonium bromide were added and the reaction mixture was stirred at 110 °C until 4-iodoaniline was completely consumed (GC-MS analysis). Then 34 mL (300 mmol) of iodobutane were added, and heating was continued for 3 days. Afterwards, the solution was poured onto 500 mL water and extracted by ethyl acetate

until the aqueous layer was colorless. The combined organic layers were washed with water (3×200 mL) and brine (2×100 mL), dried over sodium sulfate, filtered and concentrated. Purification by column chromatography (hexane) yielded 23.26 g (60%) of the product **1b** as colorless oil.

^1H NMR (200 MHz, CDCl_3) δ 7.39 (d, $J = 8.9$ Hz, 2H), 6.40 (d, $J = 9.0$ Hz, 2H), 3.23 (t, $J = 7.4$ Hz, 2H), 3.08 (d, $J = 7.3$ Hz, 2H), 1.66–1.60 (m, 1H), 1.58–1.11 (m, 12H), 1.04–0.74 (m, 9H). ^{13}C NMR (50 MHz, CDCl_3) δ 147.94, 137.56, 114.49, 75.48, 55.29, 51.60, 37.42, 30.72, 28.79, 28.36, 23.98, 23.21, 20.33, 14.13, 14.01, 10.82. Anal. Calcd for $\text{C}_{18}\text{H}_{30}\text{IN}$: C, 55.81; H, 7.81; N, 3.62. Found: C, 55.96; H, 7.33; N, 3.51.

4-(4-(*N,N*-Dibutylamino)phenyl)-2-methylbut-3-yn-2-ol (**2a**)

To a solution of 3.43 g (10.36 mmol) of *N,N*-dibutyl-4-iodobenzeneamine (**1a**) in 100 mL of degassed dry triethylamine under argon atmosphere, 1.21 g (14.37 mmol) of 2-methylbut-3-yn-2-ol, 0.038 g (0.20 mmol) of copper(I)iodide and 0.146 g (0.21 mmol) of bis(triphenylphosphine)palladium(II) dichloride ($\text{PdCl}_2(\text{btp})$) were added and the reaction mixture was stirred at 40 °C. The progress of the reaction was monitored by TLC and GC-MS analysis. After the entire conversion of **1a**, the red colored solution was filtered off, the solid residue was washed with ethyl acetate (3×100 mL) and the volatile compounds were removed *in vacuo*. The crude product was dissolved in 100 mL of ethyl acetate and extracted with water (3×100 mL) and brine (1×100 mL).

The combined organic layers were dried over sodium sulfate, filtered and concentrated. Purification by column chromatography (PE: EE = 20:3) yielded 2.63 g (88%) of **2a** as light yellow, highly viscous liquid.

^1H NMR (CDCl_3): (ppm) = 7.24 (d, J = 8.80 Hz, 2H), 6.53 (d, J = 9.00 Hz, 2H), 3.26 (t, J = 7.72 Hz, 4H), 2.11 (s, 1H), 1.60 (s, 6H) 1.64-1.48 (m, 4H), 1.43-1.25 (m, 4H), 0.95 (t, J = 7.24 Hz, 6H). ^{13}C NMR (CDCl_3): 148.02, 132.95, 111.24, 108.27, 91.31, 83.31, 65.87, 50.76, 31.84, 29.45, 20.42, 14.10.

4-(4-(Butyl-(2-ethylhexyl)amino)phenyl)-2-methylbut-3-yn-2-ol (**2b**)

2b was obtained from **1b** according to the procedure described for **1a** as a highly viscous orange liquid with a yield of 85%.

^1H NMR (200 MHz, CDCl_3) δ 7.22 (d, J = 8.9 Hz, 2H), 6.52 (d, J = 8.9 Hz, 2H), 3.26 (t, J = 7.4 Hz, 2H), 3.13 (d, J = 7.3 Hz, 2H), 2.06 (s, 1H), 1.70-1.58 (m, 1H), 1.58 (s, 6H), 1.43 - 1.11 (m, 12H), 0.95-0.83 (m, 9H). ^{13}C NMR (50 MHz, CDCl_3) δ = 148.21, 132.72, 111.57, 108.13, 91.22, 83.14, 65.74, 55.12, 51.46, 37.51, 31.71, 30.68, 28.75, 28.49, 23.95, 23.16, 20.29, 14.08, 13.96, 10.79. Anal. Calcd for $\text{C}_{23}\text{H}_{37}\text{NO}$: C, 80.41; H, 10.86; N, 4.08; Found: C, 80.23; H, 10.98; N, 4.21.

4-(Ethyne)-N,N-dibutylbenzeneamine (**3a**)

0.58 g (10.42 mmol) of dry KOH powder were added to a solution of 2.22 g (7.71 mmol) of alcohol **2a** in 100 mL of dry and degassed toluene under argon atmosphere. The suspension was heated to reflux and the acetone formed was continuously removed (the progress of the reaction was monitored by TLC and GC-MS). The mixture was then cooled to room temperature. The solid residue was filtered off and the solution was washed with water (3 \times 100 mL) and brine (1 \times 100 mL). The combined organic layers were dried over sodium sulfate, filtered off and the solvent was evaporated. The crude product was purified by column chromatography (PE: EE = 40:1) giving 1.54 g (87%) of **3a** as pale yellow, highly viscous oil.

^1H NMR (CHCl_3): δ (ppm) = 7.33 (d, J = 9.00 Hz, 2H), 6.54 (d, J = 9.00 Hz, 2H), 3.27 (t, J = 7.72 Hz, 4H), 2.96 (s, 1H), 1.64-1.49 (m, 4H), 1.44-1.26 (m, 4H), 0.96 (t, J = 7.23 Hz, 6H); ^{13}C NMR (CDCl_3): 148.33, 133.47, 111.15, 107.52, 85.22, 74.52, 50.78, 29.45, 20.43, 14.11.

N-Butyl-N-(2-ethylhexyl)-4-ethynylbenzeneamine (**3b**)

3b was obtained from **2b** according to the procedure described for **3a**. The residue was purified by column chromatography (PE: EE = 40:1) giving the product (80%) as light yellow oil.

^1H NMR (200 MHz, CDCl_3) δ 7.36 (d, J = 8.9 Hz, 2H), 6.60 (d, J = 8.9 Hz, 2H), 3.34 (t, J = 7.4 Hz, 2H), 3.20 (d, J = 7.3 Hz, 2H), 2.98 (s, 1H), 2.02 - 1.71 (m, 1H), 1.69 - 1.21 (m, 12H), 1.12 - 0.63 (m, 9H). ^{13}C NMR (50 MHz, CDCl_3) δ 148.55, 133.29, 111.57, 107.65, 85.09, 74.52, 55.20, 51.54, 37.59, 30.75, 28.82, 28.56, 24.01, 23.25, 20.36, 14.16, 14.03, 10.85. Anal. Calcd for $\text{C}_{20}\text{H}_{31}\text{N}$: C, 84.15; H, 10.95; N, 4.91. Found: C, 84.33; H, 10.75; N, 4.83.

Bis(4-((4-(dibutylamino)phenyl)ethynyl)phenyl)methanone (**B3BP**) (**5a**)

0.43 g (1.01 mmol) of **4a** and 14 mg of bis(triphenylphosphine) palladium (II) dichloride [$\text{PdCl}_2(\text{btp})$] (0.02 mmol) were dissolved in a three-neck flask in 30 mL of degassed dry THF under argon atmosphere. Then 0.57 g (2.49 mmol) of **3a**, 30 mL of degassed dry triethylamine and 3.8 mg (0.02 mmol) of copper(I)iodide were added successively. The reaction mixture was stirred at 80 $^\circ\text{C}$. The progress of the reaction was monitored by TLC. The red solution was poured onto 200 mL water and extracted by ethyl acetate until the aqueous layer was colorless. The combined organic layers were washed with water (3 \times 50 mL) and brine (2 \times 50 mL), dried over sodium sulfate, filtrated and concentrated. Purification by column chromatography (PE: CHCl_3 = 1:2) yielded 0.29 g (45%) of product as yellow powder. Mp: 67-68 $^\circ\text{C}$. ^1H NMR (200 MHz, CDCl_3) δ 7.75 (d, J = 8.2 Hz, 4H), 7.56 (d, J = 8.2 Hz, 4H), 7.38 (d, J = 8.7 Hz, 4H), 6.58 (d, J = 8.9 Hz, 4H), 3.28 (t, J = 7.3 Hz, 8H), 1.63-1.49 (m, 8H), 1.45 - 1.18 (m, 8H), 0.93 (t, J = 7.2 Hz, 12H). ^{13}C NMR (50 MHz, CDCl_3) δ 195.24, 148.32, 135.77, 133.16, 130.89, 130.00, 128.85, 111.19, 107.96, 94.76, 86.92, 50.68, 29.36, 20.32, 14.04. Anal. Calcd for $\text{C}_{45}\text{H}_{52}\text{N}_2\text{O}$: C, 84.86; H, 8.23; N, 4.40; Found: C, 84.60; H, 8.08; N, 4.28.

2,7-Bis((4-(dibutylamino)phenyl)ethynyl)-9H-fluoren-9-one (**B3FL**) (**5b**)

5b was prepared from **3a** and **4b** according to the procedure described for **5a**. Purification by column chromatography (PE: EE = 40:1) yielded the product **5b** as red crystals with a yield of 57%. Mp: 158-159 $^\circ\text{C}$. ^1H NMR (200 MHz, CDCl_3) δ 7.73 (d, J = 1.4 Hz, 2H), 7.57 (dd, J = 7.8, 1.4 Hz, 2H), 7.42 (d, J = 7.8 Hz, 2H), 7.34 (d, J = 8.8 Hz, 4H), 6.56 (d, J = 8.9 Hz, 4H), 3.31 - 3.23 (t, J = 7.3 Hz, 8H), 1.71 - 1.46 (m, 8H), 1.33-1.25 (m, 8H), 0.95 (t, J = 7.2 Hz, 12H). ^{13}C NMR (50 MHz, CDCl_3) δ 192.84, 148.17, 142.45, 137.13, 134.41, 133.00, 126.95, 125.32, 120.29, 111.18, 108.08, 93.19, 86.71, 50.68, 29.36, 20.31, 13.99. Anal. Calcd for $\text{C}_{45}\text{H}_{50}\text{N}_2\text{O}$: C, 85.13; H, 7.94; N, 4.41;. Found: C, 85.24; H, 7.81; N, 4.46.

3,6-Bis((4-(dibutylamino)phenyl)ethynyl)-9H-fluoren-9-one (**3,6-B3FL**) (**5c**)

5c was prepared from **3a** and **4c** according to the procedure described for **5a**. Purification by column chromatography (PE: CHCl_3 = 1:3) yielded the product **5c** as red crystals with a yield of 36%. Mp: 126-127 $^\circ\text{C}$. ^1H NMR (200 MHz, CDCl_3) δ 7.56 (s, 2H), 7.52 (s, 2H), 7.34 (s, 2H), 7.32 (d, J = 8.8 Hz, 4H), 6.52 (d, J = 8.8 Hz, 4H), 3.12 (t, J = 7.4 Hz, 8H), 1.51 (m, 8H), 1.29 (m, 8H), 0.90 (t, J = 7.2 Hz, 6H). ^{13}C NMR (50 MHz, CDCl_3) δ 193.17, 148.41, 143.83, 133.25, 132.89, 131.81, 130.89, 124.14, 122.80, 111.19, 107.79, 95.57, 87.58, 50.69, 29.35, 20.31, 13.99. Anal. Calcd for $\text{C}_{45}\text{H}_{50}\text{N}_2\text{O}$: C, 85.13; H, 7.94; N, 4.41;. Found: C, 85.02; H, 8.06; N, 4.19.

2,6-Bis((4-(dibutylamino)phenyl)ethynyl)anthracene-9,10-dione (**B3AN**) (**5d**)

5d was prepared from **3a** and **4d** according to the procedure described for **5a**. Purification by column chromatography

(PE: CHCl₃ = 2:5) gave the product **5d** as dark red solid with a yield of 35%. Mp: 243-244 °C. ¹H NMR (200 MHz, CDCl₃) δ 8.34 (d, *J* = 1.6 Hz, 2H), 8.23 (d, *J* = 8.1 Hz, 2H), 7.80 (dd, *J* = 8.1, 1.7 Hz, 2H), 7.38 (d, *J* = 8.8 Hz, 4H), 6.58 (d, *J* = 8.9 Hz, 4H), 3.32 - 3.24 (t, *J* = 7.3 Hz, 8H), 1.57 (m, 8H), 1.45 - 1.16 (m, 8H), 0.95 (t, *J* = 7.2 Hz, 12H). ¹³C NMR (50 MHz, CDCl₃) δ 182.27, 148.72, 135.72, 133.57, 133.25, 131.30, 130.99, 129.51, 127.33, 111.18, 107.44, 97.16, 86.88, 50.70, 29.34, 20.31, 13.99. Anal. Calcd for C₄₆H₅₀N₂O₂: C, 83.34; H, 7.60; N, 4.23; Found: C, 83.48; H, 7.45; N, 4.11.

2,7-Bis((4-(butyl(2-ethylhexyl)amino)phenyl)ethynyl)-9H-fluoren-9-one (BB3FL) (5e)

5e was prepared from **3b** and **4b** according to the procedure described for **5a**. Purification by column chromatography (PE: CHCl₃ = 2:3) gave the product **5e** as red crystals with a yield of 58%. Mp: 67-68 °C. ¹H NMR (200 MHz, CDCl₃) δ 7.73 (d, *J* = 1.4 Hz, 2H), 7.56 (dd, *J* = 7.8, 1.3 Hz, 2H), 7.42 (d, *J* = 7.8 Hz, 2H), 7.34 (d, *J* = 8.7 Hz, 4H), 6.58 (d, *J* = 8.9 Hz, 4H), 3.30 (t, *J* = 7.3 Hz, 4H), 3.17 (d, *J* = 7.2 Hz, 4H), 1.94 - 1.65 (m, 2H), 1.65 - 1.12 (m, 24H), 1.09 - 0.75 (m, 18H). ¹³C NMR (50 MHz, CDCl₃) δ 192.85, 148.49, 142.46, 137.15, 134.42, 132.90, 126.96, 125.34, 120.29, 111.65, 108.11, 93.17, 86.73, 55.15, 51.50, 37.57, 30.68, 28.75, 28.53, 23.95, 23.18, 20.31, 14.10, 13.98, 10.80. Anal. Calcd for C₅₃H₆₆N₂O: C, 85.20; H, 8.90; N, 3.75; Found: C, 85.17; H, 8.62; N, 3.79.

2,6-Bis((4-(butyl(2-ethylhexyl)amino)phenyl)ethynyl)anthracene-9,10-dione (BB3AN) (5f)

5f was prepared from **3b** and **4d** according to the procedure described for **5a**. Purification by column chromatography (PE: CHCl₃ = 1:3) gave the product **5f** as dark red solid with a yield of 40%. Mp: 184-185 °C. ¹H NMR (200 MHz, CDCl₃) δ 8.34 (d, *J* = 1.5 Hz, 2H), 8.23 (d, *J* = 8.1 Hz, 2H), 7.80 (dd, *J* = 8.2, 1.6 Hz, 2H), 7.38 (d, *J* = 8.8 Hz, 4H), 6.60 (d, *J* = 8.9 Hz, 4H), 3.31 (t, *J* = 7.3 Hz, 4H), 3.18 (d, *J* = 7.2 Hz, 4H), 1.87 - 1.66 (m, 2H), 1.66 - 1.14 (m, 24H), 1.08 - 0.76 (m, *J* = 10.4, 7.2 Hz, 18H). ¹³C NMR (50 MHz, CDCl₃) δ 182.28, 148.91, 135.74, 133.58, 133.30, 131.30, 131.00, 129.52, 127.34, 111.65, 107.46, 97.14, 86.89, 55.14, 51.49, 37.58, 30.67, 28.74, 28.53, 23.94, 23.17, 20.30, 14.09, 13.96, 10.79. Anal. Calcd for C₅₄H₆₆N₂O₂: C, 83.68; H, 8.58; N, 3.61; Found: C, 83.51; H, 8.63; N, 3.49.

Photophysics

Cyclohexane (>99.5%, Sigma-Aldrich), butyl ether (99 + %, Acros), ethyl ether (99.9% spectrophotometric grade, Sigma-Aldrich), butyl acetate (≥99.0%, Fluka), propyl acetate (99%, Alfa Aesar) and dichloromethane (>99.9%, Sigma-Aldrich) were used as received. Both in absorption as well as emission measurements the pure solvents were measured separately and the corresponding spectra were used as background.

For optical absorption spectroscopy, a Cary 50 UV/vis spectrophotometer from Varian was used, and steady-state luminescence spectra were measured with a Horiba Fluorolog-3 (JobinYvon) or a Cary Eclipse (Varian) instrument. The emis-

sion spectra were corrected using a correction function obtained from secondary fluorescence standards.⁴¹

For fluorescence decay measurements with subnanosecond time resolution, samples were excited at 395 nm with a pulsed laser diode (Picoquant, LDH-P-C-400B) and detected with a Hamamatsu photomultiplier tube. Interference and longpass filters were used to select the wavelength range for detection.

Molar extinction coefficients, ϵ , were measured in dichloromethane using 0.1 mm cuvettes. The emission quantum yields were obtained using fluorescein in basic ethanol ($\Phi_f = 0.97$)⁴² and coumarin 515 in acetonitrile ($\Phi_f = 0.67$)⁴³ as quantum counters. Samples and quantum counter solution were excited at the same wavelength, ensuring an absorption of smaller than 0.15 at and beyond the excitation wavelength.

Characterization

¹H NMR (200 MHz) and ¹³C NMR (50 MHz) spectra were measured with a BRUKER ACE 200 FT-NMR-spectrometer. The chemical shift (*s* = singlet, *bs* = broad singlet, *d* = doublet, *t* = triplet, *m* = multiplet) is stated in ppm using the nondeuterated solvent as internal standard. Solvents with a grade of deuteration of at least 99.5% were used. Melting points were measured on a Zeiss axioscope microscope with a Leitz heating block and remained uncorrected.

GC-MS runs were performed on a Thermo Scientific DSQ II using a BGB 5 column (*l* = 30 m, *d* = 0.32 mm, 1.0 μm film; achiral). Elemental microanalysis was carried out with an EA 1108 CHNS-O analyzer from Carlo Erba at the microanalytical laboratory of the Institute for Physical Chemistry at the University of Vienna.

A Ti: sapphire laser system (90 fs pulse duration, 1 kHz repetition rate) was used for the open aperture z-scan analysis. A detailed description of the setup and the fitting equations used can be found elsewhere.⁴⁴ Rhodamine B in MeOH were used as reference standards to verify the reliability of the experimental setup.⁴⁵ All PIs were prepared as 1.0 × 10⁻² M solutions in spectroscopic grade THF. The PI solutions were measured in a 0.2 mm thick flow cell in a nonrecycling volumetric flow of 4 mL/h. The excited volume is therefore refreshed approximately every 100 pulses, which approximately corresponds to 10 times for each z-position, which was found to be sufficient.

The measurements were carried out at different pulse energies in the range of 15-240 nJ. At higher energies a signal of the pure solvent appears and the solvent will contribute to the effective nonlinear absorption and even thermal effects are more likely to influence the measurement. Care had to be taken to collect the whole transmitted laser energy using a big diameter and short focal length lens. Additionally, a proper Gaussian beam profile in time and space is essential for the analysis.

TPIP Structuring Tests

Laser Device

For the direct laser writing of 3D structures, a titanium: sapphire (Ti:Sa) laser providing NIR pulses at 780 nm wavelength with a pulse duration of 100 fs is used. The system operates at

a repetition rate of 80 MHz. Direct laser writing with this system is usually carried out at a laser power below 10 mW (measured after passing the microscope objective). The laser is focused by a 100× oil immersion microscope objective (NA = 1.4), and the sample is mounted on a high-precision piezoelectric XYZ scanning stage with a 200 nm positioning accuracy.

General Procedure

For all samples the same fabrication process was implemented: The optical material was drop-cast onto a glass substrate. Subsequently, the samples were exposed to the laser beam, and the focus was scanned across the photosensitive material, which leads to an embedded 3D structure inside the material volume. After laser writing, the unexposed material was removed by development of the structure in ethanol (rinsing). The resulting structures, particularly their structural dimensions, integrity, and surface quality, were studied by means of SEM.

CONCLUSIONS

A series of aromatic ketone-based two-photon initiators containing dialkylamino groups as donors and triple bonds as conjugation bridges were successfully synthesized and evaluated. Due to the long conjugation length and good coplanarity, the evaluated initiators showed large two-photon cross section (σ_{TPA}) values, with strongly solvent dependent fluorescence lifetimes and quantum yields. With suitably strong absorption at the desired wavelength of 400 nm, the 2-, 7-substituted fluorenone-based PI **B3FL** had the highest σ_{TPA} value (440 GM) among the studied PIs. In terms of the two-photon polymerization structuring test, PIs based on fluorenone as electron withdrawing functional group with good coplanarity showed broader processing windows than that possessing benzophenone or anthraquinone moieties. Significantly better results were obtained compared to commercially available initiators and also a slight improvement in relative to well-known highly active initiators from the literature. The introduction of branched-alkyl chains significantly improved the solubility of the fluorenone-based PIs, but also slightly decreased the processing windows due to the lower migration ability of the PI with the increase of its molecular size. **B3FL** turned out to be the best performing initiator among the presented initiators, having the broadest ideal structuring process windows and good solubility in the resin. While high reactivity could be obtained in TPIP with PI concentrations as low as 0.1% wt, the novel PIs are surprisingly stable under one photon condition and nearly no photo initiation activity was found in classical photo DSC experiments.

The authors acknowledge the financial support by the China Scholarship Council (CSC), Swiss SNF, Austrian Science Fund (FWF), and the Austrian Research Agency (FFG) under Contracts N703 (STRUCMAT ISOTEC) and P18623 N-17.

REFERENCES AND NOTES

1 Rumi, M.; Barlow, S.; Wang, J.; Perry, J. W.; Marder, S. R. *Adv Polym Sci* 2008, 213, 1–95.

2 Moon, J. H.; Yang, S. *Chem Rev* 2009, 110, 547–574.

3 Park, S.-H.; Yang, D.-Y.; Lee, K.-S. *Laser Photon Rev* 2009, 3, 1–11.

4 Maruo, S.; Nakamura, O.; Kawata, S. *Opt Lett* 1997, 22, 132–134.

5 Belfield, K. D.; Schafer, K. J.; Liu, Y.; Liu, J.; Ren, X.; Stryland, E. W. V. *J Phys Org Chem* 2000, 13, 837–849.

6 Ren, Y.; Yu, X.-Q.; Zhang, D.-J.; Wang, D.; Zhang, M.-L.; Xu, G.-B.; Zhao, X.; Tian, Y.-P.; Shao, Z.-S.; Jiang, M.-H. *J Mater Chem* 2002, 12, 3431–3437.

7 Belfield, K. D.; Schafer, K. J.; Liu, Y.; Liu, J.; Ren, X.; Van Stryland, E. W. *J Phys Org Chem* 2000, 13, 837–849.

8 Belfield, K. D.; Ren, X.; Van Stryland, E. W.; Hagan, D. J.; Dubikovsky, V.; Miesak, E. J. *J Am Chem Soc* 2000, 122, 1217–1218.

9 Schafer, K. J.; Hales, J. M.; Balu, M.; Belfield, K. D.; Van Stryland, E. W.; Hagan, D. J. *J Photochem Photobiol A* 2004, 162, 497–502.

10 Pond, S. J. K.; Rumi, M.; Levin, M. D.; Parker, T. C.; Beljonne, D.; Day, M. W.; Brédas, J.-L.; Marder, S. R.; Perry, J. W. *J Phys Chem A* 2002, 106, 11470–11480.

11 Martineau, C.; Lemerrier, G.; Andraud, C.; Wang, I.; Bouriau, M.; Baldeck, P. L. *Synth Met* 2003, 138, 353–356.

12 Cumpston, B. H.; Ananthavel, S. P.; Barlow, S.; Dyer, D. L.; Ehrlich, J. E.; Erskine, L. L.; Heikal, A. A.; Kuebler, S. M.; Lee, I. Y. S.; McCord-Maughon, D.; Qin, J.; Röckel, H.; Rumi, M.; Wu, X. L.; Marder, S. R.; Perry, J. W. *Nature* 1999, 398, 51–54.

13 Xing, J.-F.; Chen, W.-Q.; Dong, X.-Z.; Tanaka, T.; Fang, X.-Y.; Duan, X.-M.; Kawata, S. *J Photochem Photobiol A* 2007, 189, 398–404.

14 He, G. S.; Tan, L.-S.; Zheng, Q.; Prasad, P. N. *Chem Rev* 2008, 108, 1245–1330.

15 Nguyen, K. A.; Rogers, J. E.; Slagle, J. E.; Day, P. N.; Kannan, R.; Tan, L.-S.; Fleitz, P. A.; Pachter, R. *J Phys Chem A* 2006, 110, 13172–13182.

16 Ramakrishna, G.; Goodson, T. *J Phys Chem A* 2007, 111, 993–1000.

17 Marder, S. R.; Torruellas, W. E.; Blanchard-Desce, M.; Ricci, V.; Stegeman, G. I.; Gilmour, S.; Bredas, J.-L.; Li, J.; Bublitz, G. U.; Boxer, S. G. *Science* 1997, 276, 1233–1236.

18 Norman, P.; Luo, Y.; Ågren, H. *Opt Commun* 1999, 168, 297–303.

19 Kamada, K.; Ohta, K.; Iwase, Y.; Kondo, K. *Chem Phys Lett* 2003, 372, 386–393.

20 Iwase, Y.; Kamada, K.; Ohta, K.; Kondo, K. *J Mater Chem* 2003, 13, 1575–1581.

21 Pucher, N.; Rosspeintner, A.; Satzinger, V.; Schmidt, V.; Gescheidt, G.; Stampfl, J. R.; Liska, R. *Macromolecules* 2009, 42, 6519–6528.

22 Rumi, M.; Ehrlich, J. E.; Heikal, A. A.; Perry, J. W.; Barlow, S.; Hu, Z.; McCord-Maughon, D.; Parker, T. C.; Röckel, H.; Thayumanavan, S.; Marder, S. R.; Beljonne, D.; Brédas, J.-L. *J Am Chem Soc* 2000, 122, 9500–9510.

- 23** Rosspeintner, A.; Griesser, M.; Pucher, N.; Iskra, K.; Liska, R.; Gescheidt, G. *Macromolecules* 2009, 42, 8034–8038.
- 24** Liu, J.; Gao, F.; Yang, L.; Wang, C.; Li, H.; Zhang, S. *Chem Lett* 2010, 39, 324–325.
- 25** Belfield, K. D.; Bondar, M. V.; Przhonska, O. V.; Schafer, K. *J. Photochem Photobiol Sci* 2004, 3, 138–141.
- 26** Belfield, K. D.; Bondar, M. V.; Yanez, C. O.; Hernandez, F. E.; Przhonska, O. V. *J Mater Chem* 2009, 19, 7498–7502.
- 27** Corredor, C. C.; Belfield, K. D.; Bondar, M. V.; Przhonska, O. V.; Yao, S. *J Photochem Photobiol A* 2006, 184, 105–112.
- 28** Estrada, L. A.; Neckers, D. C. *J Org Chem* 2009, 74, 8484–8487.
- 29** Takalo, H.; Kankare, J.; Hanninen, E. *Acta Chem Scand Ser B* 1988, B42, 448–454.
- 30** Suh, S. C.; Suh, M. C.; Shim, S. C. *Macromol Chem Phys* 1999, 200, 1991–1997.
- 31** Michel, P.; Gennet, D.; Rassat, A. *Tetrahedron Lett* 1999, 40, 8575–8578.
- 32** Gouloumis, A.; Gonzalez-Rodriguez, D.; Vazquez, P.; Torres, T.; Liu, S.; Echegoyen, L.; Ramey, J.; Hug Gordon, L.; Guldi Dirk, M. *J Am Chem Soc* 2006, 128, 12674–12684.
- 33** Abashev, G. G.; Lebedev, K. Y.; Osorgina, I. V.; Shklyeva, E. V. *Russ J Org Chem* 2006, 42, 1873–1876.
- 34** Novikov, A. N.; Slyusarchuk, V. T.; Chaikovskaya, L. G. (Tomsk Polytechnic Institute, USSR; Tomsk Medical Institute). *SU 642288 A1* 19790115, 1979.
- 35** Ipaktschi, J.; Hosseinzadeh, R.; Schlaf, P.; Dreiseidler, E.; Goddard, R. *Helv Chim Acta* 1998, 81, 1821–1834.
- 36** Bhatt, M. V. *Tetrahedron* 1964, 20, 803–821.
- 37** The majority of the observed fluorescence decays were monoexponential. For 3,6-B3FL in BE and EE, as well as B3BP in BE biexponential decays with a fast component have been observed. These short components may tentatively be attributed to emission from the locally excited state.
- 38** Fujiwara, T.; Lee, J.-K.; Zgierski, M. Z.; Lim, E. C. *Phys Chem Chem Phys* 2009, 11, 2475–2479.
- 39** Sheik-Bahae, M.; Said, A. A.; Wei, T. H.; Wu, Y. Y.; Hagan, D. J.; Soileau, M. J.; Van Stryland, E. W. *Proc SPIE-Int Soc Opt Eng* 1990, 1148, 41–51.
- 40** Heller, C.; Pucher, N.; Seidl, B.; Kalinyaprak-Icten, K.; Ullrich, G.; Kuna, L.; Satzinger, V.; Schmidt, V.; Lichtenegger, H. C.; Stampfl, J.; Liska, R. *J Polym Sci Part A: Polym Chem* 2007, 45, 3280–3291.
- 41** Gardecki, J. A.; Maroncelli, M. *Appl Spectrosc* 1998, 52, 1179–1189.
- 42** Martin, M. M. *Chem Phys Lett* 1975, 35, 105–111.
- 43** Jones, G.; Jackson, W. R.; Choi, C. Y.; Bergmark, W. R. *J Phys Chem* 1985, 89, 294–300.
- 44** Ajami, A.; Husinsky, W.; Liska, R.; Pucher, N. *J Opt Soc Am B: Opt Phys* 2010, 27, 2290–2297.
- 45** Makarov, N. S.; Drobizhev, M.; Rebane, A. *Opt Express* 2008, 16, 4029–4047.